LAMINAR-TURBULENT TRANSITION CORRELATION IN SUPERSONIC/HYPERSONIC FLOW - ATTACHED VERSUS SEPARATED FLOW

George A. Simeonides
Hellenic Aerospace Industry, Tanagra, Schimatari, Greece

Keywords: *transition, supersonic, hypersonic, flat plate, cone, bluntness, separation*

Abstract

The previously correlated attached supersonic/ hypersonic flow transition onset data is compared to data from regions of shock wave boundary layer interaction, where transition is found to be efficiently promoted through the associated flow reattachment process. In order to isolate interaction effects and to verify minimum transition Reynolds numbers (which are shown to be potentially more than an order of magnitude lower than in attached flow), additional carefully designed experiments are necessary. The correlated attached flow data is used to identify transition Reynolds number trends with Mach number and bluntness Reynolds number, while discrepancies with flight data over cones remain unexplained and/ or partially explained. In this regard, well documented investigations in quiet tunnels and flight, explicitly addressing also bluntness effects, are appreciated.

List of symbols

b	leading edge or nose bluntness
M	Mach number
Re_b	bluntness Reynolds number $= \dfrac{\rho u b}{\mu}$
Re_{xtrans}	transition onset Reynolds number $= \dfrac{\rho u x_{tr}}{\mu}$
	(based on local flow conditions)
T	temperature
u	stream-wise velocity
x	stream-wise distance from the leading edge

Greek symbols

α	angle of attack
μ	viscosity
ρ	density

Subscripts

e	boundary layer edge
rec	recovery / adiabatic wall
tr	transition onset location
w	wall conditions
0	total (stagnation) flow conditions

Superscript

$*$	Eckert's reference enthalpy conditions (density and viscosity)

1 Introduction

Further to the reasonably successful correlation of a significant number of flat plate, cone and complete vehicle configuration (along the windward symmetry line) transition data in supersonic and hypersonic attached flow conditions [1-4], the well observed phenomenon of transition promotion by shock wave boundary layer interactions [5-9] is put into scrutiny, viz a viz the previous findings for attached flows.

Section 2 presents a brief overview of the correlation effort of [1-4] for attached flow transition, followed by a summary of transition promotion observations through regions of shock boundary layer interaction [5-9]. Section 3 examines additional cone transition data from the review work of [10,13], and presents alternative forms of the correlation of [4] to better illustrate anticipated transition trends with Mach number and bluntness (Reynolds number). Section 4 elaborates on the findings of transition promotion by shock wave boundary layer interaction for comparison with attached flow transition data in section 5. The results are summarized in section 6.

2 Background

2.1 Attached flow transition correlation

The findings of [1-4] for transition in attached high speed flows are summarized in Fig. 1 [4], with (Re_b/M^2) as the independent variable and $M(x_{tr}/b)$ as the dependent variable (both based on local boundary layer edge flow conditions).
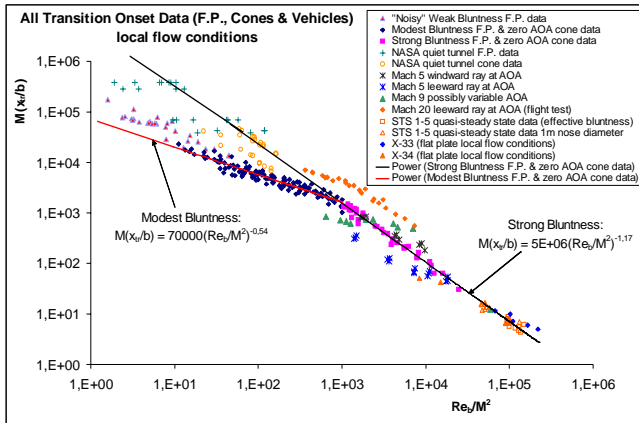
Fig. 1 Complete set of transition onset data in the proposed correlation form (local flow conditions) [4]

The flat plate data in Fig. 1 has been taken from 11 references, covering a range in free-stream-based leading edge bluntness Reynolds number, Re_b, between 20 and 100,000 and in free-stream-based transition onset Reynolds number, Re_{xtrans}, between 0.7 and 20 million, for free-stream Mach numbers between 2 and 8 [3,4].

The cone transition data has been taken from 6 references, and covers a range in free-stream-based leading edge bluntness Reynolds number, Re_b, between 360 and 2.7 million and in free-stream-based transition onset Reynolds number, Re_{xtrans}, between 1.9 and 44 million, for free-stream Mach numbers between 3.5 and 20 [4].

In addition, Fig. 1 includes STS 1-5 Space Shuttle flight transition data and some transition data over the X-33 and X-34 vehicle configurations [4].

The main conclusions from the correlation effort of [4] have been:

1. The "strong bluntness correlation" of the form:

$$Re_{xtrans} = 5 \cdot 10^6 M^{1.34} Re_b^{-0.17} \qquad (1)$$

represents the data for $Re_b/M^2 > 1000$, and also the "high stability" data in the range $Re_b/M^2 < 1000$.

2. At $Re_b/M^2 < 1000$, the majority of the (generally weak / modest bluntness nose / leading edge, wind tunnel) data exhibits reduced stability and an important role of flow disturbance parameters; in this data range, the lower transition bound is closely represented by the "modest bluntness correlation":

$$Re_{xtrans} = 70,000 M^{0.08} Re_b^{0.46} \qquad (2)$$

3. The effect of (small) angle of attack on transition over slender (conical) configurations deserves further attention (see e.g. [10]); for example on the leeward side, angle of attack has been found to have a destabilizing effect in the Mach 5 cone wind tunnel experiments of [15], and an opposite stabilizing effect in the Mach 20 flight test data of [16], Fig. 1. In all cases, cone transition data, affected by angle of attack, diverges significantly from eq. (1) in Fig. 1.

2.2 Transition promotion by separated / reattaching flow (shock wave boundary layer interaction)

The work of [5-9] as well as investigations by other authors, e.g. [11,12], on supersonic and hypersonic shock wave boundary layer interactions have shown that the reattaching boundary layer downstream of the interaction zone exhibits significant disturbance amplification in the form of Goertler vortices. It has also become evident that these instabilities, closely linked with the adverse pressure gradient and flow concavity through the reattachment process, are very effective in the promotion of laminar-turbulent transition in flow situations that would otherwise (in the absence of the interaction, e.g. over an undisturbed flat plate) have remained fully laminar or transitioned more slowly, as illustrated by the streamwise heat transfer distributions in Fig. 2 [5,6].
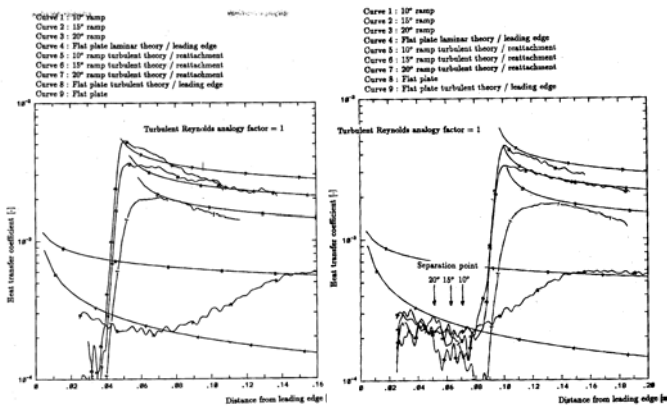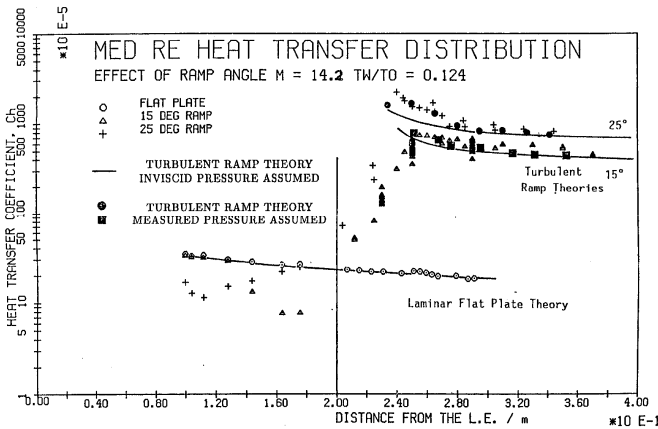
Fig. 2 Heat transfer distributions over flat plate and flat plate / ramp configurations at Mach 14 (upper) and Mach 6 (lower), exhibiting transition promotion by shock wave boundary layer interaction [5,6]

Furthermore, a peak heating correlation was established in [5-9], focusing at the time on the prediction of the peak heating level encountered just downstream of reattachment in regions of shock wave boundary layer interaction (Fig. 3). This correlation provides interesting insight to the promotion of laminar-turbulent transition in such flow situations, illustrating that transition may be effectively triggered by the interaction / flow reattachment process beyond a critical reference Reynolds number.

The correlation of Fig. 3 [5-9] includes approximately 200 data points from 23 references that cover a range in freestream Mach number between 5 and 20, five orders of magnitude in reference Reynolds number and a wide variety of two- and three-dimensional laminar, transitional and fully turbulent shock wave boundary layer interactions. The majority of the (hypersonic) data in Fig. 3 is characterized by "cold" (ambient temperature)

wall, perfect gas flow, intermittent wind tunnel conditions, and involves nominally sharp (weak/modest bluntness) leading edge configurations with a flat plate forebody, corresponding to the less stable data on the left half of Fig. 1.
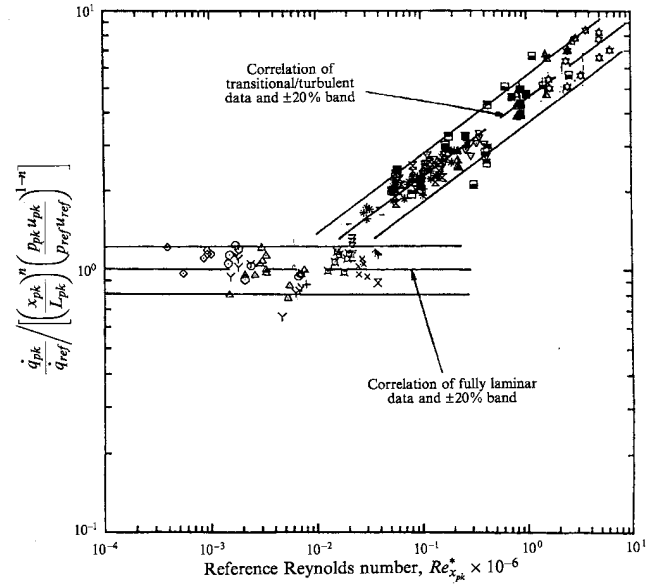
Fig. 3 Correlation of laminar and turbulent shock boundary layer interaction heat transfer data referenced to laminar flat plate heating [5-9]

3 Further Analysis of Attached Flow Transition Data

3.1 Additional literature on attached flow transition (cones and angle of attack effects)

Schneider [10,13] has performed extensive surveys of available transition data, particularly over (sharp and blunt) cones, from both wind tunnel and flight experiments.

With respect to the aforementioned angle of attack effect on transition onset over cones, the following observations are noted in [10]:
1. Transition on both sharp and blunt cones is very sensitive to small angle of attack, especially for slender cones with smaller nose bluntness. They both appear to exhibit cross-flow instability at angle of attack.
2. Transition over sharp cones at angle of attack moves aft on the windward ray and forward on the leeward ray compared to the zero angle of attack case (see also [14] for a proposed correlation of angle of attack effects on transition over sharp cones).

3. Over blunt cones, transition at angle of attack also moves aft on the windside and forward on the leeside, for small bluntness.
4. With large bluntness, the effect of angle of attack reverses and transition moves forward on the windside and aft on the leeside.

The distinction, however, between small and large bluntness with respect to the observed reversal in the angle of attack effect on transition, and also the causes for such reversal, remain unclear and deserve further investigation. Still, what can be observed at this time in Fig. 1, is that, with increasing nose bluntness (from a nose diameter of 1.4 mm to a nose diameter of 17.5 mm [15], and from 5 mm to up to 20 mm [16]), transition on the leeside of the respective cones shifts as follows: in the case of the data of [15], from an initially forward location and low $M(x_{tr}/b)$ values (with respect to the zero angle of attack situation and the strong bluntness correlation, eq. (1)) towards eq. (1); in the case of the data of [16], from an initial location correlating reasonably well with zero angle of attack data and eq. (1), towards significantly higher $M(x_{tr}/b)$ values than predicted by eq. (1).

Furthermore, published flight data for laminar-turbulent transition is summarized in [13], including a tabulation of the data of [17,18] in the well known plot of transition Reynolds number on "sharp" cones in wind tunnels and flight versus Mach number, Fig. 4 [19]. The excessive data scatter in Fig. 4 has been explained in [20,24] with the help of stability analysis and e^N results, and data has been found to correlate when wall cooling and Mach number effects on transition over sharp cones are accounted for.

It is noted, however, in [13] that the so-called "sharp" cones that provided the data for this plot were not all really sharp, and that angle of attack in many cases was not zero; these parameters are likely to have played an important role, too, in the data scatter observed in Fig. 4, but availability of the relevant information (that could allow for a more appropriate data re-processing) is limited in the literature. This should be kept in mind when the flight data of Fig. 4 is compared to the data used

in the correlation of Fig. 1 [4] in the next section.
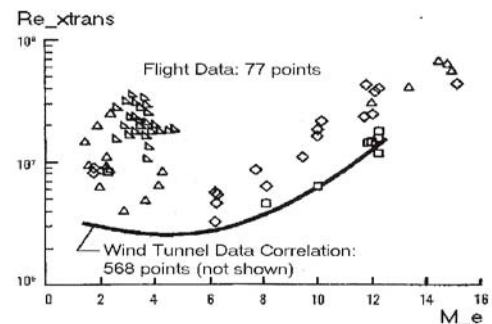
Fig. 4 Flight (symbols) and mean wind tunnel (solid line) transition Reynolds number data over "sharp" cones [19]

Lastly, the thorough cone transition experiments, including flight tests at transonic / low supersonic Mach numbers [25], deserve special attention. Here, angles of attack and sideslip were carefully controlled and maintained to +/- 0.2 degrees (thus reported to have a small effect on the measured transition locations), while nose bluntness is identified as less than 100 μm. The measured transition Reynolds numbers have also been corrected to adiabatic wall conditions.

3.2 Attached flow transition correlation revisited

The strong bluntness correlation of the data in Fig. 1, eq. (1), may also take the form:

$$\frac{\text{Re}_{xtrans}}{M} = 5 \cdot 10^6 \left(\frac{\text{Re}_b}{M^2} \right)^{-0.17} \qquad (3)$$

This correlation has been found in [4] to be representative of all "high stability" data throughout the data range of Fig. 1. In this form, it may be used to provide transition Reynolds number as a function of Mach number, with $\left(\text{Re}_b / M^2 \right)$ as a parameter.

Similarly, eq. (2), representing a correlation for "reduced stability" transition data in the weak / modest bluntness regime, may take the following form:

$$\frac{\text{Re}_{xtrans}}{M} = 70,000 \left(\frac{\text{Re}_b}{M^2} \right)^{0.46} \qquad (4)$$

The data of Fig. 1 is now plotted in Fig. 5 in the parameterization form of eqs. (3) and (4)[1]. Also shown is part of the flight data [13,17,18] for which some indication of nose bluntness is provided in the survey of [13]; this data corresponds entirely to cone and cone-cylinder configurations and may well be affected by the presence of (small) angle of attack.
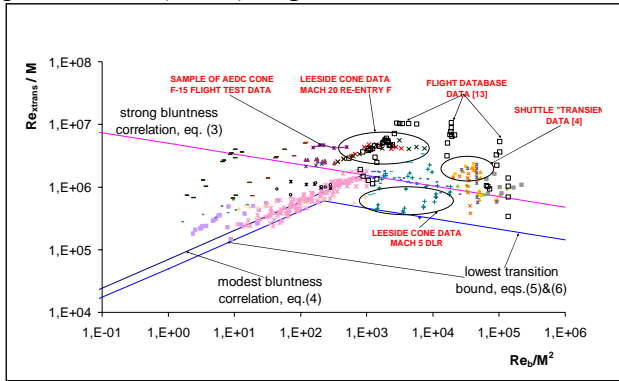
Fig. 5 Transition data [4] (local flow conditions) - alternative correlation parameters

The first observation to be made in Fig. 5 is that, despite the reasonably good representation of strong bluntness and quiet tunnel transition data by eqs. (1) and (3), a significant part of the flight test cone transition data of [13,17,18], including the Re-entry F data elaborated also in the correlation of [4] and Fig. 1, exhibits significant scatter, with transition Reynolds numbers of up to almost an order of magnitude higher than eq. (3) and an upper bound in (Re_{xtrans}/M) of approximately 10 million. In this respect, the likely influence of angle of attack on the flight data needs to be evaluated (to the extent that available information may allow it), as already discussed in [13].

Still, it is noted that preliminary evaluation (in the context of the correlation proposed in [4]) of the flight data of [25], also indicates in-flight transition Reynolds numbers that are significantly higher than predicted by eq. (3) in Fig. 5, despite the particular attention paid to angle of attack in these tests. Evidently, further investigations are needed to resolve such issues with generic configurations, and especially

cones. Nose bluntness effects should be explicitly addressed in such studies, covering a wide range in Mach and (unit/bluntness) Reynolds numbers, while particular attention should be paid to angle of attack and wall temperature effects, similar to the work of [25].

On the lower end of the observed transition Reynolds numbers in Fig. 5, the transition bound in the weak / modest bluntness regime is closely represented by a form similar to, and approximately 25% to 30% lower than the respective correlation, eq. (4). In the strong bluntness regime, the major divergence to lower values than eq. (3) is related to cone angle of attack effects. The low transition bound for all data in Fig. 5 is, then, described by eqs. (5) and (6), respectively for the weak / modest bluntness $[(\mathrm{Re}_b/M^2) < 230]$ and the strong bluntness $[(\mathrm{Re}_b/M^2) \geq 230]$ regimes:

$$\frac{\mathrm{Re}_{xtrans}}{M} = 50{,}000\left(\frac{\mathrm{Re}_b}{M^2}\right)^{0.46} \qquad (5)$$

$$\frac{\mathrm{Re}_{xtrans}}{M} = 1.5 \cdot 10^6 \left(\frac{\mathrm{Re}_b}{M^2}\right)^{-0.17} \qquad (6)$$

In order now to facilitate comparison of the entirety of the flight test data of [13,17,18], Fig. 4 (where precise nose bluntness information is not provided), and the transition data correlated in [4], Fig. 1, the plot of transition Reynolds number versus Mach number (based on local flow conditions) is presented in Fig. 6. The open square symbols, the majority of which lies on the high side of transition Reynolds number, represent the flight test data tabulated in [13].

The strong and modest bluntness correlation curves, eqs. (1) & (3) and eqs. (2) & (4) respectively, are also plotted in Fig. 6, with (Re_b) as a parameter. It is evident that eqs. (2) & (4) are a weak function of Mach number, and transition Reynolds number increases approximately as the square root of (Re_b); on the contrary, eqs. (1) & (3) yield an increasing transition Reynolds number with Mach number, which however, decreases at a modest rate with increasing (Re_b).

---

[1] The cone data from the NASA quiet tunnel [21] are modified in Fig. 5 (shifted to the right), in order to account for the actual nose bluntness (nose diameter), as opposed to the nose radius erroneously used in Fig. 1 [4].

For a given bluntness Reynolds number ($Re_b > 1000$), the transition Reynolds number first (at low / supersonic Mach numbers) increases with Mach number, in accordance with eqs. (1) & (3). When eqs. (1) & (3) intersect eqs. (2) & (4) for the corresponding bluntness Reynolds number, transition may thereafter occur at effectively a constant Reynolds number, despite any further increase in Mach number, following the trend of eqs. (2) & (4). In more stable flow situations, transition Reynolds number will continue to rise with Mach number along the "broken line" part of eqs. (1) & (3) corresponding to the given value of bluntness Reynolds number.
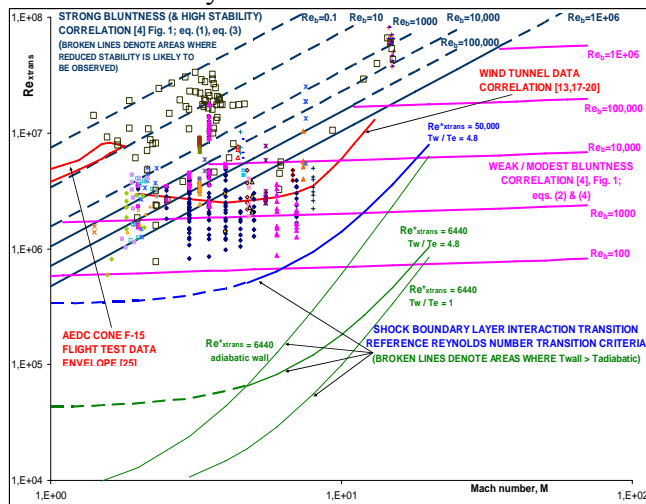
Fig. 6 Transition Reynolds number versus Mach number with bluntness Reynolds number as a parameter - attached versus separated / reattaching supersonic/hypersonic flow

Particularly at small values of the bluntness Reynolds number, Re_b, a highly stable flow environment is necessary to achieve the large transition Reynolds numbers predicted by eqs. (1) & (3); instead, the significantly lower levels of transition Reynolds number, anticipated by eqs. (2) & (4), are far more likely to be encountered in a disturbed flow wind tunnel environment around configurations with a nominally sharp (weak / modest bluntness) and, often, irregular nose / leading edge.

It is interesting to note that the flight data of [25] follows qualitatively the strong bluntness correlation trend of transition Reynolds number with Mach number, although quantitatively it falls above the predictions of eq. (3) for the corresponding bluntness Reynolds numbers

(typically around 1000). Also, the wind tunnel data of [25] exhibits, at least qualitatively, the modest bluntness correlation, eq. (4), trends of Fig. 5.

With reference to Fig. 7 (and the more detailed presentation provided in Fig. 10 of [3]), this is probably the reason for the well known "transition reversal" trend observed in ground experiments with increasing bluntness (Reynolds number). In fact, in nominally sharp / small bluntness cases, transition usually occurs at low Reynolds numbers, dominated by the high disturbance wind tunnel environment. According to the modest bluntness correlation (which is only a weak function of Mach number), eqs. (2) & (4), transition Reynolds number increases with bluntness (Reynolds number), until a critical value of the bluntness Reynolds number where, for the given Mach number, the trend switches to the strong bluntness correlation and transition Reynolds number decreases thereafter with any further increases in Re_b.

Figure 7 also indicates that, should there be no effect of sharp leading edge irregularities and the typical high disturbance environment of standard wind tunnels, very high transition Reynolds numbers could be anticipated over sharp / weak bluntness configurations, decreasing monotonically with increasing bluntness Reynolds number for any given supersonic / hypersonic Mach number.
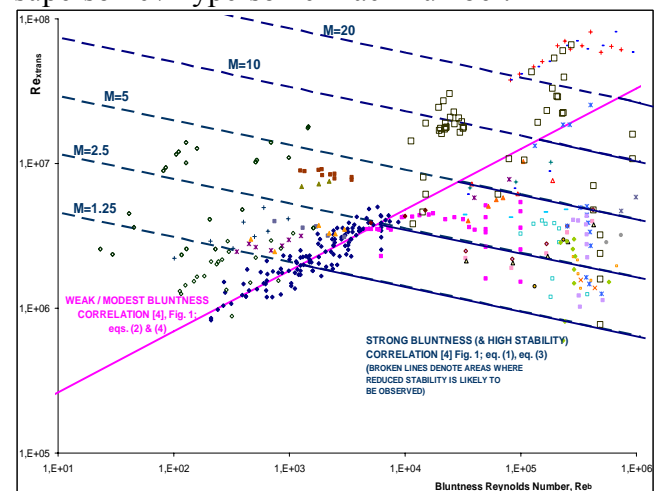
Fig. 7 Transition Reynolds number versus bluntness Reynolds number, with Mach number as a parameter

4 Elaboration of Separated Flow Transition Results in the Peak Heating Correlation

Scrutinizing Fig. 3, in accordance with the peak heating correlation parameters identified in detail in [5], a reference Reynolds number of 6440 (based on the flat plate forebody flow conditions, just upstream of the interaction) is found to be the theoretically critical value for transition promotion by the shock wave boundary layer interaction process: at lower reference Reynolds numbers, one finds that the turbulent heat transfer rate would be theoretically lower than the corresponding laminar heat transfer rate! However, the bound between some fully laminar interaction data and the majority of the available turbulent peak heating data has been found in practice at moderately higher reference Reynolds numbers (above 20,000).

For a perfect gas, and assuming a power temperature-viscosity law approximation, the relation between Reynolds number and reference Reynolds number is [22]:

$$\mathrm{Re}_{xtrans} = \mathrm{Re}^*_{xtrans}\left(\frac{T^*}{T_e}\right)^{(1+\omega)} \qquad (7)$$

where the exponent ω ranges between 0.65 and 1, with a typical value of 0.76.

Using Eckert's [23] reference temperature definition:

$$T^*/T_e = 0.28 + 0.50 \cdot T_w/T_e + 0.22 \cdot T_{rec}/T_e$$

with $T_{rec}/T_e = 1 + r\dfrac{\gamma-1}{2}M^2$, $\gamma=1.4$ and $r=0.85$

for the laminar oncoming flow, eq. (7) becomes:

$$\mathrm{Re}_{xtrans} = \mathrm{Re}^*_{xtrans}\left(1+0.0374M^2+0.5\left(\frac{T_w}{T_e}-1\right)\right)^{1.76} \qquad (8)$$

Indicatively, equation (8) reduces to:

$$\mathrm{Re}_{xtrans} = \mathrm{Re}^*_{xtrans}\left(1+0.0374M^2\right)^{1.76} \qquad (8a)$$
$$\text{for } T_w=T_e$$

$$\mathrm{Re}_{xtrans} = \mathrm{Re}^*_{xtrans}\left(1+0.1224M^2\right)^{1.76} \qquad (8b)$$
$$\text{for } T_w=T_{rec} \text{ (adiabatic wall)}$$

$$\mathrm{Re}_{xtrans} = \mathrm{Re}^*_{xtrans}\left(2.9+0.0374M^2\right)^{1.76}$$
for $T_w=4.8T_e$ (e.g. hypersonic wind tunnel conditions over a flat plate, $\qquad$ (8c)
$T_w=288$ K; $T_e=60$ K)

It is noted that, at approximately Mach 4.75, the condition of eq. (8c) becomes identical to the adiabatic wall condition, eq. (8b), while it is recalled that Fig. 3 includes data in the Mach number range (upstream of the interaction) between 5 and 20. As Mach number increases, eq. (8c) approaches eq. (8a) because of the high velocity content of the total enthalpy.

From the preceding analysis, and once the critical transition reference Reynolds number is identified from the data of Fig. 3, transition Reynolds number criteria for areas of shock wave boundary layer interaction may be established as a function of the Mach number, with the wall-to-boundary layer edge temperature ratio as a parameter. It is noted that, in this case, the resulting transition Reynolds number is based on the flow conditions approaching the interaction and not on the local flow conditions just downstream of reattachment where transition actually occurs.

5 Comparison of Attached and Separated Flow Transition Results

5.1 Transition Reynolds number versus Mach number

Shown in Fig. 6 are also eqs. (8a) thru (8c), representing the transition (reference) Reynolds number for the cases of shock wave boundary layer interaction of Fig. 3. The most representative relation for the data of Fig. 3 is eq. (8c), corresponding to $T_w=4.8T_e$, shown in Fig. 6 for the (theoretically, in accordance with Fig. 3) critical transition reference Reynolds number, $Re^*_{xtrans}=6440$, and for an arbitrarily selected value of $Re^*_{xtrans}=50,000$. For Mach numbers below approximately 4.75, where the wall temperature condition of eq. (8c) effectively implies a heated wall to temperatures above the adiabatic wall level, the curves representing eq. (8c) are shown as broken lines.

The effectiveness of shock wave boundary layer interaction in promoting laminar-turbulent transition becomes evident in Fig. 6. At the value of the critical reference Reynolds number, $Re^*_{xtrans}=6440$, and in the Mach number range 5 to 8, where a large amount of data is available for both attached and separated flow, transition Reynolds number (based on forebody flow conditions upstream of the interaction) may be more than one order of magnitude lower than the previously found lower bound for attached flow transition. Even for a value of Re^*_{xtrans} of $50,000$, above which the majority of the turbulent reattaching data has been collected in Fig. 3 [9], transition is found to occur at significantly lower Reynolds numbers than in the most unstable weak bluntness attached flow cases.

In order to illustrate better the effect of shock wave boundary layer interaction on laminar-turbulent transition promotion, Fig. 5 is reproduced as Fig. 8. Here, only the "core" attached flow data (modest and strong bluntness) is included, as used to establish the correlation forms in [3,4], the NASA quiet tunnel data [21] (reasonably represented by the strong bluntness correlation) and the weak bluntness data (that is scattered between the modest and strong bluntness correlation curves at low Re_b/M^2 values); cone transition data that is likely to have been affected by angle of attack and the Shuttle transient transition data [4] is excluded from Fig. 8.
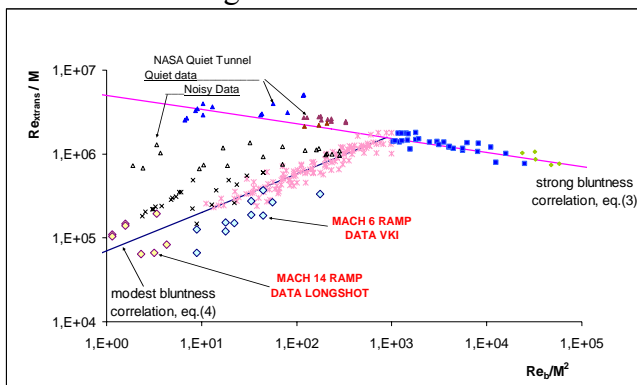
Fig. 8 Transition data - attached versus separated / reattaching flow

Figure 8 also incorporates the Mach 6 and Mach 14 shock wave boundary layer interaction transition data from Fig. 3, for which leading edge bluntness information is available [5]. The relevant correlation parameters are again based on flow conditions over the flat plate upstream of the interaction and not over the deflected ramp where transition occurs. The entirety of this data falls in the weak / modest bluntness regime. Moreover, it corresponds to reference Reynolds numbers in Fig. 3 between 20,000 and 200,000, i.e. significantly higher than the theoretically critical reference Reynolds number value of 6440.

Nevertheless, with reference to Fig. 2, it is noted that although it has not been possible to produce laminar-turbulent transition over a flat plate at zero incidence within the available Reynolds number range at Mach 14 (Re_x/M of up to 350,000), transition was efficiently promoted on the deflected ramp just downstream of reattachment in all cases. The same holds also for the Mach 6 cases tested with thicker leading edges (exhibiting the higher Re_b/M^2 values in Fig. 8), as illustrated in Fig. 9. Moreover, it is seen in the Mach 6 cases of Fig. 2, corresponding to the sharper leading edge experiments, that although transition is occurring along the flat plate, its extent to fully turbulent flow is significantly longer than in the case of reattaching flow over the various (10, 15 and 20-degree) deflected ramps.
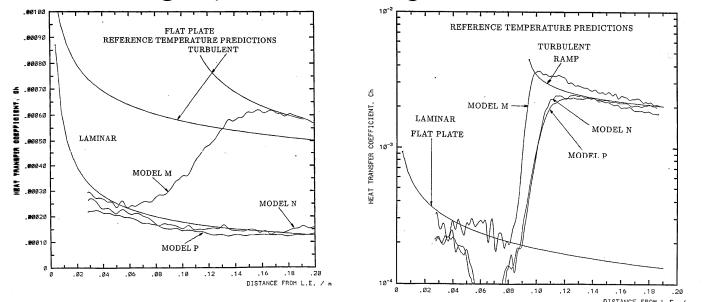
Fig. 9 Heat transfer distributions over flat plate (left) and shock boundary layer interaction (right) - effect of leading edge thickness [5] (Model M: 40μm; Model N: 98 μm; Model P: 316 μm)

Taking the above into account, specifically that the recorded transition Reynolds numbers in the reattachment region are not necessarily the minimum possible values, it is observed in Fig. 8 that the majority of the Mach 6 data falls well below the modest bluntness correlation curve, eq. (4), and also below the corresponding lowest transition bound for attached flow, eq. (5). The

same is true for part of the Mach 14 data. With regard to the Mach 14 cases, for which reattaching flow transition falls above the modest bluntness correlation curve in Fig. 8, it should be kept in mind that transition over the flat plate alone was not possible in the Mach 14 experiments, even at higher Reynolds numbers.

5.2 Are local flow conditions through the interaction sufficient to correlate transition promotion with attached flow data?

If, now, the shock wave boundary layer interaction transition data incorporated in Fig. 8 is transformed to local flow conditions over the ramp (at the actual transition location), the data is shifted to higher values of Re_b/M^2 and closer to the modest bluntness correlation curve, as shown in Fig. 10. This is due to the significant drop in Mach number and the change in unit Reynolds number caused by the flow deflection over the 15 and 25 degree ramps used in the tests. Alternatively, if only the ordinate parameter in Fig. 10, characterizing the transition onset location, is transformed to local flow conditions over the ramp (still, using the full running length of the boundary layer from the model leading edge to the transition onset location), while the independent variable in the abscissa remains based on the upstream flow conditions over the flat plate, the data is shifted above the modest bluntness correlation.
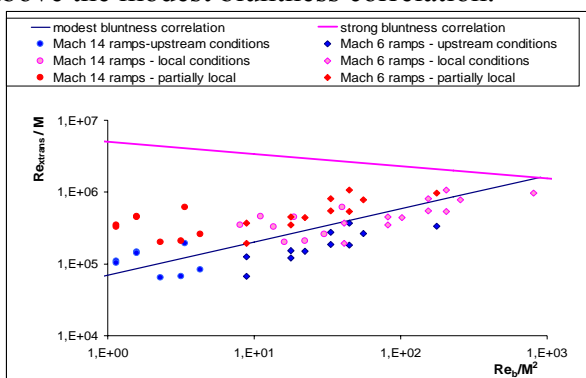
Fig. 10 Effect of local flow conditions on hypersonic ramp transition correlation parameters

These observations tend to indicate that transition promotion through shock boundary layer interactions might be macroscopically approximated just by accounting for the change in local flow conditions, irrespective of the

case-specific destabilizing mechanisms of flow concavity, adverse pressure gradient, boundary layer thinning and Goertler vortices. In this regard, it will be interesting to compare shock boundary layer interaction data, e.g. over flat plate / ramp configurations, exhibiting transition in the reattachment region, with transition onset measurements over flat plates at angle of attack (wedge flow), with equivalent local flow conditions and leading edge bluntness.

6 Summary and Conclusions

From the preceding discussion, the following observations can be made with respect to attached flow transition:

1. The correlation of [4] provides reasonable approximation to a significant number of data and insight to transition trends, but underestimates much of the flight data over cones.
2. There is a need for carefully designed and well documented quiet tunnel and flight experiments, such as [25], especially with regard to the characterization of combined nose bluntness and angle of attack effects on transition over cones, covering a wide Mach and Reynolds number range (and also wall temperature effects).
3. On the basis of eqs. (3) & (4), increasing bluntness Reynolds number has a strong stabilizing effect in "reduced stability" cases, and a (smaller) destabilizing effect in "high stability" and strong bluntness cases. Increasing Mach number has a significant stabilizing effect in "high stability" cases, and a nearly neutral influence in "reduced stability" cases, which are particularly evident at small bluntness Reynolds numbers. These trends are, at least qualitatively, consistent with the flight and wind tunnel data of [25].

With respect to shock wave boundary layer interactions, the process of reattachment is found to promote laminar-turbulent transition, effectively reducing the transition Reynolds number (based on the approaching flow conditions), indicatively by a factor of 2 and potentially by more than an order of magnitude

relative to the most unstable attached flow data of [4]. More work is required here to isolate interaction effects (e.g. comparing transition over ramps to wedges), and also to better quantify bluntness effects.

References

[1] Simeonides G (1996) Leading edge bluntness effects on flat plate boundary layer transition - compilation of high speed experimental data. ESA-ESTEC Doc. YPA/1881/GS, included in ESA-ESTEC EWP-1880

[2] Simeonides G (2003) Correlation of laminar-turbulent transition data over flat plates in supersonic / hypersonic flow including leading edge bluntness effects. *Shock Waves Journal*, Vol. 12, No. 6, Springer, pp. 497-508

[3] Simeonides G (2004) Laminar-turbulent transition correlations in supersonic / hypersonic flat plate flow. *24th ICAS Congress*, Yokohama, Japan

[4] Simeonides G & Kosmatopoulos E (2006) Laminar-turbulent transition correlation in supersonic/hypersonic flow. *25th ICAS Congress*, Hamburg, Germany

[5] Simeonides G (1992) Hypersonic shock wave boundary layer interactions over compression corners. Ph. D. Thesis, U. Bristol/von Karman Inst.

[6] Vermeulen JP & Simeonides G (1992) Parametric studies of shock wave boundary layer interactions over 2D compression corners at Mach 6. von Karman Institute TN 181

[7] Simeonides G (1993) Hypersonic shock wave boundary layer interactions over simplified deflected control surface configurations. AGARD-FDP/VKI Special Course, AGARD Report 792

[8] Simeonides G & Haase W (1995) Experimental and computational investigations of hypersonic flow about compression ramps. *Journal Fluid Mechanics*, Vol. 283, pp. 17-42

[9] Simeonides G (1996) Laminar-turbulent transition promotion in regions of shock wave boundary layer interaction. *MSTP Code Validation Workshop, Manned Space Transportation Programme*, ESTEC, Noordwijk, The Netherlands. Included in ESA-ESTEC EWP-1880

[10] Schneider S P (2004) Hypersonic laminar-turbulent transition on circular cones and scramjet forebodies. *Progress in Aerospace Sciences*, Vol. 40, Elsevier

[11] Ginoux JJ (1969) On some properties of reattaching laminar and transitional high speed flows. von Karman Institute TN 53

[12] Delery J (1989) Shock/shock and shock wave boundary layer interactions in hypersonic flows. AGARD Report 761

[13] Schneider S P (1999) Flight data for boundary layer transition at hypersonic and supersonic speeds. *AIAA J. Spacecraft and Rockets*, Vol. 36, No. 1, pp. 8-20

[14] Yushin A Ya (1982) Influence of the angle of attack on the transition from a laminar to a turbulent boundary layer in the case of supersonic flow past sharp circular cones. *Fluid Dynamics,* Vol. 17, No. 4, pp. 160-163, Nauka/Interperiodica, distributed by Springer Science & Business Media

[15] Schoeler H & Banerji A (1983) Visualization of boundary layer transition on a cone with liquid crystals, *ICIASF '83 Record of International Congress on Instrumentation in Aerospace Simulation Facilities*

[16] Wright RL & Zoby EV (1987) Flight Boundary Layer Transition Measurements on a Slender Cone at Mach 20, *AIAA 10th Fluid & Plasma Dynamics Conference,* Albuquerque, New Mexico

[17] Beckwith I E (1975) Development of a high Reynolds number quiet tunnel for transition research. *AIAA Journal*, Vol. 13, No. 3, pp. 300-306

[18] Beckwith I E & Bertram M H (1972) A survey of NASA Langley studies on high speed transition and the quiet tunnel. NASA TM-X-2566

[19] Stetson K F (1992) Hypersonic boundary layer transition. *Advances in Hypersonics: Defining the Hypersonic Environment*, Birkhauser, pp. 324-417 (also 2nd Joint Europe / US Short Course in Hypersonics, U.S. Air Force Academy, 1989)

[20] Malik M R (1989) Prediction and control of transition in supersonic and hypersonic boundary layers. *AIAA Journal*, Vol. 27, No. 11, pp. 1487-1493

[21] Chen F.J., Malik M.R. and Beckwith I.E. (1989) Boundary layer transition on a cone and flat plate at Mach 3.5. *AIAA Journal*, Vol. 27, No. 6, pp. 687-693

[22] Hirschel EH (2004) Basics of aerothermodynamics. Springer & AIAA

[23] Eckert ERG (1955) Engineering relations of friction and heat transfer to surfaces in high velocity flow. *J. Aero. Sciences*, Vol. 22, No. 8

[24] Reshotko E (2008) Transition prediction – supersonic and hypersonic flows. RTO-AVT-VKI Lecture Series *Advances in Laminar-Turbulent Transition Modelling*, von Karman Institute

[25] Fisher D F & Dougherty N S (1982) Flight and wind tunnel correlation of boundary layer transition on the AEDC transition cone. NASA TM 84902

Copyright Statement